ACS Chemical Neuroscience

Research Article

pubs.acs.org/chemneuro

Synthesis of a FTO Inhibitor with Anticonvulsant Activity

Guanqun Zheng,[†] Thomas Cox,[‡] Leah Tribbey,[‡] Gloria Z. Wang,[†] Paulina Iacoban,[‡] Matthew E. Booher,[∥] Gregory J. Gabriel,[∥] Lu Zhou,[⊥] Nancy Bae,[§] Joie Rowles,[‡] Chuan He,[†] and Mark J. Olsen*[,‡]

[†]Department of Chemistry, University of Chicago, 929 E. 57th St., Chicago, Illinois 60637, United States

[‡]Department of Pharmaceutical Sciences, College of Pharmacy − Glendale, and [§]Department of Biochemistry, Arizona College of Osteopathic Medicine, Midwestern University, 19555 N. 59th Ave., Glendale, Arizona 85308, United States

[∥]Department of Chemistry and Biochemistry, Kennesaw State University, 1000 Chastain Rd., Box 1203, Kennesaw, Georgia 30144, United States

[⊥]School of Pharmacy, Fudan University, 826 Zhangheng Rd., Shanghai 201203, P. R. China

ABSTRACT: We describe the rationale for and the synthesis of a new class of compounds utilizing a modular approach that are designed to mimic ascorbic acid and to inhibit 2-oxoglutarate-dependent hydroxylases. Preliminary characterization of one of these compounds indicates in vivo anticonvulsant activity (6 Hz mouse model) at nontoxic doses, inhibition of the 2-oxoglutarate-dependent hydroxylase FTO, and expected increase in cellular N^6-methyladenosine. This compound is also able to modulate various microRNA, an interesting result in light of the recent view that modulation of microRNAs may be useful for the treatment of CNS disease.

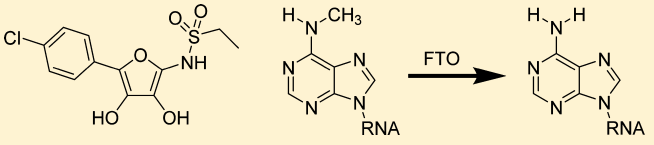

KEYWORDS: *Anticonvulsant, FTO, N^6-methyladenosine, RNA, microRNA, epilepsy*

Epilepsy is a chronic disorder of abnormal electrical activity in the brain characterized by recurrent unprovoked seizures.[1] Treatment with traditional antiepileptic drugs (AEDs) is not effective for about 30% of patients, and pharmaco-resistant epilepsy remains a current clinical challenge. Agents that modify the disease progression, antiepileptogenics,[2] may have some advantages over traditional AEDs. Recently, the need for novel agents for the treatment of pharmaco-resistant epilepsy and the development of antiepileptogenics has been emphasized.[3−5]

We sought to design and synthesize novel antiepileptogenic compounds that induce the production of erythropoietin (Epo) in the CNS. Our rationale was based on reports of the neuroprotective[6] and antiepileptogenic effects[7] of Epo. Additionally, Epo has been demonstrated to induce beneficial mood swings in patients suffering from depression,[8,9] which is the most frequent comorbidity with epilepsy.[10] Developing a single agent with both antiepileptogenic and antidepressant effects would enhance value as a novel agent for the treatment of epilepsy.

Epo production is controlled through the HIF (hypoxia inducible factor) pathway.[11] HIF proteins are transcription factors that control the expression of hypoxia-induced genes to overcome the crisis of hypoxia. The enzyme prolyl-4-hydroxylase 2 (PHD2) has a critical role in this pathway by targeting HIF-1α for proteasomal degradation; this enzyme is active under usual, nonhypoxic conditions. PHD2 is a member of a family of oxygen-requiring, 2-oxoglutarate (2-OG) dependent hydroxylases that utilize nonheme iron in the catalytic site and ascorbic acid as cofactor.[12] We have recently proposed an antiepileptogenic mechanism in which inhibition of PHD would permit HIF proteins to function and to induce the expression of Epo and other hypoxia-induced genes.[1] Therefore, our rational drug design was to inhibit PHD which would lead to increased endogenous expression of Epo in the CNS. Our compounds did not, however, inhibit PHD but rather a related enzyme family member, FTO (fat mass and obesity). We describe the synthesis and initial characterization of this FTO inhibitor and demonstrate anticonvulsant activity in an animal model of pharmaco-resistant epilepsy.[3,4]

We selected the aminohydroxyfuranone core (**1**, Figure 1) as a scaffold for developing PHD inhibitors due to the similarity to ascorbic acid (**2**, Figure 1) which is known to have antioxidant[13,14] and PHD-binding properties.[15] Tetronic acid derivatives (**3**, Figure 1) are related to ascorbic acid and have

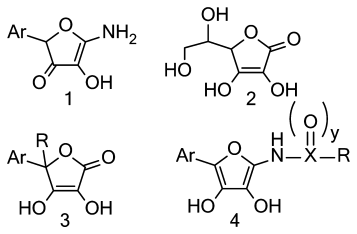

Figure 1. Scaffold selection for prolyl-4-hydroxylase inhibitors based upon a core dihydroxyfuran moiety. X = C or S, y = 1 or 2. **1**, aminohydroxyfurananones; **2**, ascorbic acid; **3**, arylhydroxytetronic acids; **4**, 2,5-disubstituted-3,4-dihydroxyfurans.

Received: February 25, 2014
Revised: April 30, 2014
Published: May 18, 2014

been shown to significantly inhibit cyclooxygenase and lipoxygenase,[16] activities that might be desirable to modulate the neuroinflammation that occurs during epileptogenesis.[17] However, the scaffold of **3** does not readily permit for the elaboration of additional functional groups for PHD inhibition. We reasoned that adding an additional functional group to the terminal amine of **1** to yield a 2,5-disubstituted 3,4-dihydroxyfuran scaffold, **4**, would result in a family of ascorbic acid mimics that would also be able to mimic 2-OG due to the presence of an amide or sulfonamide. Compounds from scaffold **4** still resemble ascorbic acid, allowing for the potential for these high polar surface area compounds to utilize the sodium-coupled vitamin C transporters 1 and 2 (SVCT1 and 2) for blood-brain barrier (BBB) penetration. Ascorbic acid mimics that are capable of utilizing transporters may resolve the conundrum of developing BBB-penetrating 2-OG mimics, due to the strong negative charge of 2-OG needed for recognition of the PHD active site, yet simultaneously possessing an appropriate log *P* and low polar surface area characteristics required of BBB penetrating agents (see below). These compounds may also target other related enzymes such as FIH, ASPH, TET-1, and FTO.

The crystal structure of PHD2[18] provided crucial information for our drug design by revealing specific molecular interactions between the 2-OG ligand, the critical active site iron, and Arg383 that is involved in 2-OG recognition. The 2,5-disubstituted 3,4-dihydroxyfuran scaffold enables a modular approach to developing PHD inhibitors as illustrated in Figure 2. The concept was to position an aryl group as module A

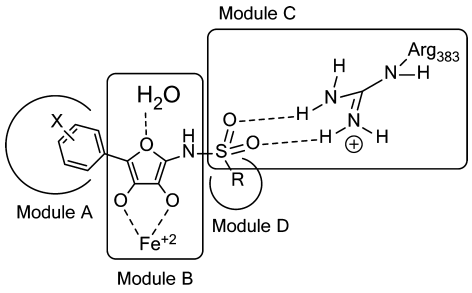

Figure 2. Conceptual design of prolyl-4-hydroxylase inhibitor utilizing a modular approach with a core dihydroxyfuran moiety.

which is tolerated in known PHD2 inhibitors.[19] In module B, the aminohydroxyfuranone ring core can serve as an iron chelating moiety to interact with the active site Fe and also provide a hydrogen bond acceptor to a critically positioned water molecule.[18] Module C is a carbonyl or sulfonyl adaptor to serve as a hydrogen bond acceptor for Arg383, as well as a synthetic handle for attaching Module D. The presence of different modules is expected to result in different 2-oxoglutarate/ascorbic acid mimics with different enzyme inhibition selectivities.

RESULTS AND DISCUSSION

Synthesis of the targeted compounds is illustrated in Scheme 1. The synthesis begins with the condensation of potassium cyanide, glyoxal bisulfite addition product, and an aryl aldehyde originally explored by Dahn and co-workers,[20] and is followed by an acetylation or sulfonylation to give compounds **6** and **7**. Acetylation with acetic anhydride results exclusively in the *O*-acetyl product **6b**, while reaction with methylsulfonyl chloride and ethylsulfonyl chloride result in both **6c** and **7c**, the result of O- and N-sulfonylation, respectively. Reaction with phenylsulfonyl chloride results exclusively in the **6e** O-sulfonylation product. The compounds synthesized are indicated in Table 1.

Table 1. Prepared Compounds

compd	X	*y*	R
5			
6b	C	1	CH_3
6e	S	2	C_6H_5
7c	S	2	CH_3
7d	S	2	CH_2CH_3

Computational methods were utilized to evaluate the feasibility and potential metabolic liability of proposed compounds prior to synthesis. Selected physicochemical and biological properties were calculated using StarDrop version 5.3.1 build 202, and are shown in Tables 2 and 3. These calculations indicate that the compounds **7c** and **7d** have solubility and log *P* values that are consistent with good BBB

Table 2. Calculated Physicochemical Properties

compd	MW	TPSA (Å^2)[a]	log *S*	log *P*
5	225.6	72.5	3.93	1.07
6b	267.6	78.6	2.90	1.07
6e	365.7	95.7	1.33	1.67
7c	303.6	99.8	3.28	1.74
7d	317.6	99.8	3.08	2.11

[a]Total polar surface area.

Table 3. Predicted Biological Activities

compd	BBB	log(BB)	Cyp3A4	Cyp2D6	hERG pIC_{50}
5	+	−0.03	0.85	medium	3.83
6b	−	0.11	0.82	medium	3.68
6e	−	−0.13	0.75	medium	4.27
7c	−	−0.18	0.64	low	5.05
7d	−	−0.15	0.51	medium	5.18

Scheme 1[a]

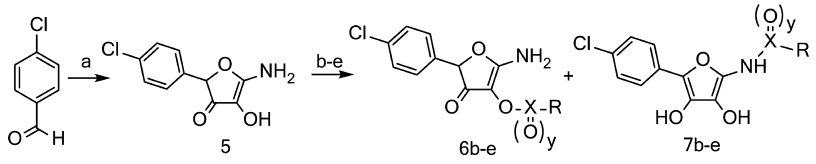

[a](a) KCN, glyoxal bisulfite addition product, Na_2CO_3; (b) Ac_2O, RT; (c) K_2CO_3, $ClSO_2CH_3$, THF, reflux; (d) K_2CO_3, $ClSO_2CH_2CH_3$, THF, reflux; (e) K_2CO_3, $ClSO_2C_6H_5$, THF, reflux.

dx.doi.org/10.1021/cn500042t | ACS Chem. Neurosci. 2014, 5, 658−665

penetration, but have polar surface area values that are above what is usually considered favorable for passive diffusion across the BBB. However, compounds with similar high polar surface areas have been reported to cross the BBB by utilization of the SVCT2.[21] Since the dihydroxyfurans mimic ascorbic acid, it is reasonable to predict that they may penetrate the BBB via SVCT2.

Biological screening of perspective antiepileptogenic compounds is extremely challenging, and there is no generally accepted series of experiments to evaluate antiepileptogenic potential. Our compounds were screened for anticonvulsant activity in mice by the NIH/NINDS/ASP, using the following models: maximal electroshock (MES), subcutaneous metrazole (scMET), and 6 Hz. The compounds showed little to no protection in the MES and scMET models (data not shown). However, most compounds were effective in the 6 Hz model (Table 4). These results clearly demonstrate in vivo anticonvulsant activity and therefore likely CNS penetration of the compounds, possibly via ascorbic acid transporters.[21] The ASP screened these compounds for general CNS toxicity using the rotarod method, and little to no toxicity was found (Table 5). Based on predicted cytochrome P450 oxidation, **7d** was selected for advancement to the quantitative 6 Hz model. Analysis using this method indicated that the **7d** anticonvulsant EC_{50} was 18 mg/kg, the toxic EC_{50} was 347 mg/kg, resulting in a safety ratio (toxic EC_{50}/anticonvulsant EC_{50}) of 19.3, indicating reasonable safety (Table 6). To put these data into perspective, **7d** had a higher safety ratio than all commercially available AEDs tested except for levetiracetam.[22] It is also interesting to note that levetiracetam, a very useful agent to treat epilepsy, was also not active in the MES and scMET models.[22]

Table 4. Activity in the 6 Hz Model

compd[a]	0.25 h[b] (*N*/*F*)[c]	0.5 h (*N*/*F*)	1 h (*N*/*F*)	2 h (*N*/*F*)	4 h (*N*/*F*)
5	1/4	0/4	1/4	1/4	0/4
6b	2/4	0/4	1/4	0/4	1/4
6e	1/4	0/4	2/4	2/4	2/4
7c	1/4	4/4	4/4	3/4	4/4
7d	1/4	3/4	2/4	3/4	3/4

[a]Compounds were injected in 0.1% methylcellulose i.p. at 100 mg/kg. [b]Time after i.p. injection. [c]*N* is the number of protected animals, and *F* is the total number of animals in trial group.

Table 5. Toxicity in the Rotarod Model

compd[a]	0.25 h[b] (*N*/*F*)[c]	0.5 h (*N*/*F*)	1 h (*N*/*F*)	2 h (*N*/*F*)	4 h (*N*/*F*)
5	0/4	0/4	0/4	0/4	0/4
6b	0/4	0/4	0/4	0/4	0/4
6e	0/4	0/4	0/4	0/4	0/4
7c	0/4	1/4	2/4	0/4	3/4
7d	0/4	0/4	0/4	1/4	0/4

[a]Compounds were injected in 0.1% methylcellulose i.p. at 100 mg/kg. [b]Time after i.p. injection. [c]*N* is the number of animals displaying toxicity, and *F* is the total number of animals in trial group.

Table 6. Activity of 7d in the Quantitative 6 Hz and Toxicity Model

test[a]	*t* (h)	dose (mg/kg)	*N*/*F*[b]
6 Hz	1.0	1.0	0/8
6 Hz	1.0	2.5	1/8
6 Hz	1.0	5.0	5/8
6 Hz	1.0	10.0	5/8
6 Hz	1.0	25.0	11/16
6 Hz	1.0	50.0	4/8
6 Hz	1.0	100.0	10/16
6 Hz	1.0	200.0	6/8
Toxicity	8.0	100.0	0/8
Toxicity	8.0	200.0	2/8
Toxicity	8.0	300.0	3/8
Toxicity	8.0	500.0	5/8
Toxicity	8.0	750.0	7/7

[a]Compound was injected in 0.1% methylcellulose i.p. [b]*N* is the number of animals displaying protection or toxicity, and *F* is the total number of animals in trial group.

Compounds **7c** and **7d** were further tested for activity in the HIF pathway. Treatment of HeLa cells with dimethyl *N*-oxalylglycine, a global inhibitor of 2-OG enzymes, inhibits PHD, stabilizes HIF1α,[23] and turns on the expression of HIF-induced genes including Epo.[24] HeLa cells were treated with or without **7c** and **7d**, and then analyzed for stabilization of HIF1α and HIF2α by Western blots. Stabilization of HIF1α or HIF2α was not seen, nor were Epo levels changed (data not shown), indicating that **7c** and **7d** do not inhibit PHD under these experimental conditions.

We considered that our compounds may be interacting with enzymes related to PHD that also utilize 2-OG. Examination of the structure of **7c** and **7d** with the conformations of the inhibitor *N*-oxalylglycine (NOG) from crystal structures of PHD,[18] FIH,[25] Jumanji-C containing histone demethylase JMJD2A,[26] and FTO[27] suggested that FTO was a reasonable target. The conformation of NOG in PHD, FIH, and JMJD2A is nearly identical, and is entirely planar as illustrated in Figure 3. In contrast, NOG from FTO is significantly twisted out of the plane, and results in O5 being nearly 1.76 Å above the plane containing the amide bond. Due to the presence of the sulfonamide in both **7c** and **7d**, a sulfone oxygen can be nearly

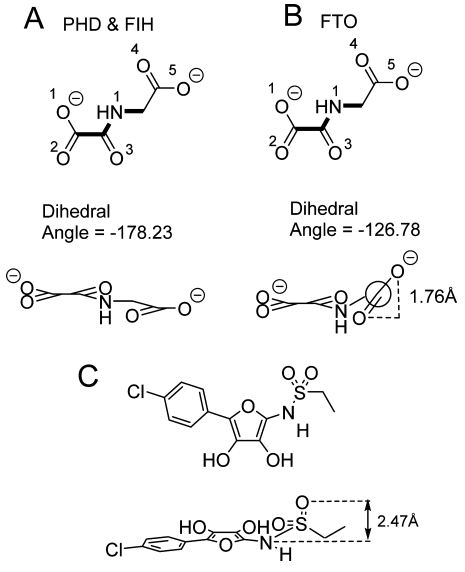

Figure 3. (A) Conformational analysis of NOG from crystal structures 3HQR and 2XUM for PHD and FIH. (B) Conformational analysis of NOG from 3LFM for FTO. (C) Conformational analysis of **7d**.

dx.doi.org/10.1021/cn500042t | ACS Chem. Neurosci. 2014, 5, 658−665

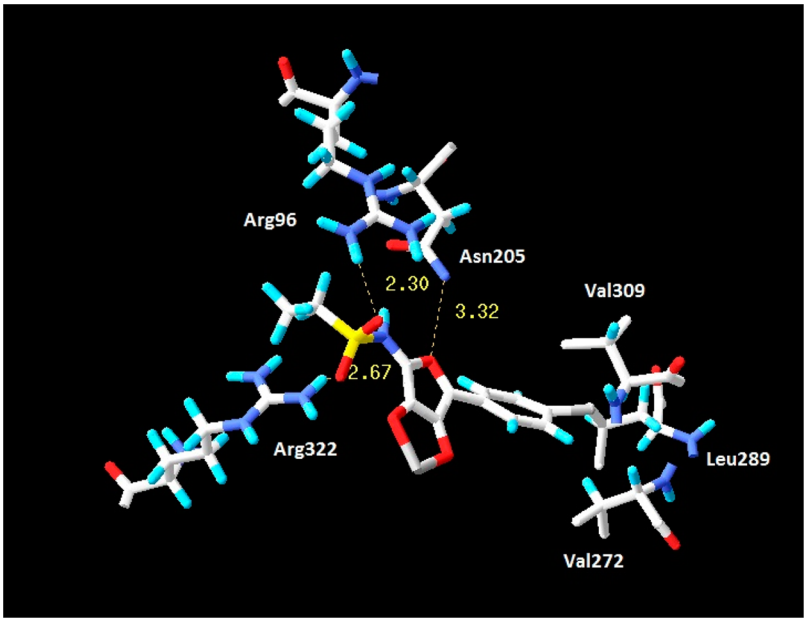

Figure 4. Computational model of **7d** binding at the active site of FTO (3LFM).

2.47 Å above the plane of the iron chelating dihydroxyfuran moiety. We hypothesized that **7c** and **7d** might inhibit FTO, and that the key distinguishing feature of FTO inhibition versus PHD inhibition is the presence of a nonplanar hydrogen bond acceptor capable of mimicking the terminal carboxylate oxygen of 2-OG at the FTO active site.

The compounds **7c** and **7d** were tested for the ability to inhibit purified FTO.[28] The results indicate that FTO was inhibited by each compound, with IC_{50}'s of 4.9 and 8.7 μM, respectively. These values are similar to those reported for broad-spectrum 2-OG oxygenase inhibitors, 3-methylthymidine (IC_{50} 8.3 μM),[29] *N*-oxalylglycine (IC_{50} 44 μM),[29] and rhein (IC_{50} 21 μM).[30] To assess the cellular effect of FTO inhibition, total HeLa cell mRNA was quantified for the presence of N^6-methyladenosine (m^6A). FTO is a nucleic acid demethylase that prefers RNA m^6A[28] over other substrates such as N^3-methyluracil and N^3-methylthymine.[31] A 9.3% increase in m^6A was observed following treatment of 25 μM **7d** ($p < 0.05$), which is very comparable to the observed increase in m^6A following FTO siRNA.[28] These results indicate that **7c** and **7d** inhibit FTO and produce the expected increase of m^6A in mRNA. A model of **7d** binding at the active site of FTO was created using the crystal structure 3LFM, as illustrated in Figure 4. The dihydroxyfuran moiety is involved in chelating the active site Fe^{2+}, while both of the sulfonamide oxygens form hydrogen bonds, one with Arg322, the other with Arg96. The oxygen of the furan ring is proposed to hydrogen bond with Asn205. This proposed recognition of the FTO active site is similar in concept to the original design for inhibiting PHD (Figure 2).

These results suggest a connection between FTO inhibition and anticonvulsant activity. We have recently proposed a functional association between FTO, RNA epigenetics and epilepsy.[32] FTO is highly expressed in neurons in the CNS, and in multiple brain regions including the hippocampus.[33] The most common mRNA modification in eukaryotes is m^6A, which, as mentioned above, is the preferred substrate for FTO. The presence of m^6A is highly enriched in brain tissue.[34] MicroRNA (miRNA) is a class of small noncoding RNA involved in silencing targeted genes. miRNAs bind to a specific region in the 3′UTR of the target mRNA to promote degradation or translation inhibition. Recently, an association between these miRNA binding sites and m^6A residues in the 3′ UTR has been described.[34,35] miRNA are known to be highly expressed in CNS tissue, and are increasingly investigated in CNS disease states including epilepsy and epileptogenesis.[36] A recent review clearly presents evidence that epilepsy and the pathological epileptogenesis mechanism involve miRNAs that control multiple genes and proteins.[37]

We reasoned that a FTO inhibitor with anticonvulsant activity that modulates m^6A may also modulate miRNA, and that modulation of miRNA may underlie the anticonvulsant and/or antiepileptogenic activity. To initially test this hypothesis, we incubated HeLa cells with **7d**, harvested total RNA, and analyzed the sample for miRNA modulation. The results of the microarray screening showed that multiple miRNAs were modulated as an effect of **7d** (Table 7). Some miRNA were up-regulated, while others were down-regulated. These results are consistent with emerging views concerning the involvement of miRNAs and epilepsy.[38] Further testing is required before any definitive mechanism of anticonvulsant

Table 7. Modulation of microRNA by 25 μM 7d

microRNA	*P*-value	log2(G2/G1)[a]
miR-6509-3p	1.94×10^{-2}	−2.73
miR-4444	4.06×10^{-2}	0.60
miR-671-5p	4.20×10^{-2}	0.35
miR-6722-5p	4.40×10^{-2}	−1.05
miR-4713-5p	5.99×10^{-2}	−1.39
miR-4638-5p	6.21×10^{-2}	1.47
miR-4717-5p	6.62×10^{-2}	−1.70
miR-6514	7.06×10^{-2}	−1.44
miR-4329	7.18×10^{-2}	−1.62
miR-4485	7.52×10^{-2}	−0.60
miR-486-3p	8.61×10^{-2}	−1.81
miR-34b-3p	8.91×10^{-2}	−1.66

[a]G2 is the signal from **7d** treated (25uM) HeLa cells, and G1 is the signal from untreated control HeLa cells.

dx.doi.org/10.1021/cn500042t | *ACS Chem. Neurosci.* 2014, 5, 658−665

activity can be made. It is noted that a common variant in the FTO gene, rs9939609, has been linked to several CNS conditions including reduced brain volume[39] and risk for alcohol dependence,[40] and that the effect of this genetic variation seems to be increased FTO protein activity.[41] Further, dopaminergic-specific FTO knockout mice display attenuated responses to cocaine.[42] These results provide evidence for the role of a FTO inhibitor in the treatment of CNS diseases.

CONCLUSIONS

Novel dihydroxyfuran sulfonamides were prepared by condensation of arylhydroxytetronimides with sulfonyl chlorides. Our modular design scheme readily permits syntheses of additional compounds that may show specificity to unique 2-OG-dependent enzymes. The rationale was to develop novel agents for epilepsy by inhibiting PHD with subsequent increased production of Epo.[1] While the synthesized compounds do not appear to inhibit PHD, this result does not refute the potential role of a PHD inhibitor for epilepsy therapy. We found that several novel compounds inhibited the closely related enzyme, FTO, which also utilizes Fe^{2+} and 2-OG at the active site. The molecule, **7d**, has anticonvulsant activity in the 6 Hz mouse model at nontoxic doses, inhibits the enzymatic activity of the RNA demethylase FTO, increases the amount of m^6A in total cellular RNA, and modulates levels of specific miRNAs. To our knowledge, this is the first FTO inhibitor that demonstrates anticonvulsant activity. Although direct measurement of BBB penetration was not performed, the demonstration of in vivo anticonvulsant activity strongly implies penetration into the CNS. A BBB-penetrating small molecule inhibitor may provide an advantage over the use of siRNA to modulate FTO. Similarly, this approach may have an advantage over antagomir-based methods to modulate miRNA that have been proposed for the treatment of epilepsy.[43] While we cannot definitively state at this time that the inhibition of FTO is the cause of the anticonvulsant activity and of the modulation of miRNA, there is considerable emerging discussion describing a functional, interdependent role of these activities.

METHODS

All chemical reagents were purchased from Sigma-Aldrich unless specified otherwise. Antibodies were purchased from Novus Biologicals (Littleton, CO). NMR data were recorded on a Bruker Avance DPX-300 MHz NMR spectrometer. All melting points are uncorrected and were performed on a Hoover melting point apparatus. Elemental analysis was performed by Atlantic Microlab, and mass spectrometry was performed by the University of Cincinnati.

Organic Synthesis. **5** and **6b** were synthesized according to literature methods.[44] **6e**, **7c**, and **7d** were prepared using the following method utilizing benzenesulfonyl chloride, methanesulfonyl chloride, and ethanesulfonyl chloride, respectively. An amount of 5 g of 5-amino-4-hydroxy-2-(4-chlorophenyl)-furan-3-one was stirred in 50 mL of dry tetrahydrofuran (THF) under nitrogen gas for 16 h with 4.7 g of K_2CO_3 and the appropriate sulfonylation reagent (1 equiv). The reaction was filtered, and the filtrate was acidified with 24 mL of 1 N HCl and then extracted five times with 20 mL of diethyl ether. The combined ether extracts were washed with brine and dried with Na_2SO_4. After filtration, 100 mL of hexanes was added to the solution, resulting in a precipitate, which was collected using vacuum filtration and recrystallized with MeOH.

*Compound **5**, 5-Amino-4-hydroxy-2-(4-chlorophenyl)-furan-3-one.* . Yield = 70%. mp 221−222 °C. FTIR 3079, 1638. ^{1}H NMR (300 MHz, DMSO-d_6, ppm) δ 7.82 (s, 2H), 7.46 (d, J = 8.7 Hz, 2H), 7.30 (s, 1H), 7.29 (d, J = 8.7 Hz, 2H), 5.43 (s, 1H). ^{13}C NMR (75 MHz, DMSO-d_6, ppm) δ 182.6, 173.1, 135.7, 133.2, 128.9, 128.6, 111.7, 82.2. HRMS Calcd: 248.00849. Found: 248.00852 MNa^+ = $C_{10}H_8NO_3ClNa^+$. Elemental Analysis Calcd: C 53.23, H 3.57, N 6.21, Cl 15.71. Found: C 53.35, H 3.61, N 6.24, Cl 15.83, $C_{10}H_8ClNO_3$. HPLC retention time: 16.7 min.

*Compound **6b**, 2-(4-Chlorophenyl)-4-(acetoxy)-5-amino-3(2H)-furanone.* Yield = 44%. mp 221−222 °C. FTIR 3030, 1628. ^{1}H NMR (300 MHz, DMSO-d_6, ppm) δ 8.30 (s, 2H), 7.47 (d, J = 8.7 Hz, 2H), 7.35 (d, J = 8.7 Hz, 2H), 5.63 (s, 1H), 2.14 (s, 3H). ^{13}C NMR (75 MHz, DMSO-d_6, ppm) δ 182.4, 173.0, 168.9, 134.8, 133.8, 129.1, 129.1, 106.9, 83.2, 20.7. Elemental Analysis Calcd: C 53.85, H 3.77, N 5.23. Found: C 53.76, H 3.90, N 5.24, $C_{12}H_{10}ClNO_4$. HPLC retention time: 19.7 min.

*Compound **6e**, 2-(4-Chlorophenyl)-4-[[phenylsulfonyl]oxy]-5-amino-3(2H)-furanone.* Yield = 17%. mp 190−195 °C. FTIR 3034, 1630. ^{1}H NMR (300 MHz, DMSO-d_6, ppm) δ 8.54 (s, 2H), 7.93 (d, J = 8.1 Hz, 2H), 7.74 (t, J = 7.2 Hz, 1H), 7.57 (t, J = 8.1 Hz, 2H), 7.48 (d, J = 8.7 Hz, 2H), 7.18 (d, J = 8.4 Hz, 2H), 5.54 (s, 1H). ^{13}C NMR (75 MHz, DMSO-d_6, ppm) δ 181.2, 173.4, 135.2, 135.0, 134.2, 133.9, 129.7, 129.2, 129.1, 129.0, 106.6, 82.9. Elemental Analysis Calcd: C 52.54, H 3.31, N 3.83, Cl 9.69. Found: C 52.50, H 3.33, N 3.79, Cl 9.84, $C_{16}H_{12}ClNO_5S$. HPLC retention time: 32.2 min.

*Compound **7c**, N-(3,4-Dihydroxy-5-(4-chlorophenyl)-2-furanyl)-methanesulfonamide.* The material was further purified by column chromatography (hexanes/ethyl acetate). Yield = 18%. mp 175 °C. FTIR 3169, 1616. ^{1}H NMR (300 MHz, DMSO-d_6, ppm) δ 8.41 (s, 1H), 8.09 (s, 1H), 7.96 (d, J = 8.4 Hz, 2H), 7.85 (s, 1H), 7.59 (d, J = 8.4 Hz, 2H), 3.55 (s, 3H). ^{13}C NMR (75 MHz, DMSO-d_6, ppm) δ 185.7, 165.1, 140.7, 136.9, 135.9, 133.5, 130.0, 129.7, 40.7. Elemental Analysis Calcd: C 43.50, H 3.32, Cl 11.67, N 4.61. Found: C 43.66, H 3.40, Cl 11.54, N 4.55, $C_{11}H_{10}ClNO_5S$. HPLC retention time: 25.2 min.

*Compound **7d**, N-(3,4-Dihydroxy-5-(4-chlorophenyl)-2-furanyl)-ethanesulfonamide.* Yield = 21%. mp 183−185 °C. FTIR 3181, 1616. ^{1}H NMR (300 MHz, DMSO-d_6, ppm) δ 8.41 (s, 1H), 8.08 (s, 1H), 7.95 (d, J = 9.3 Hz, 2H), 7.85 (s, 1H), 7.59 (d, J = 9.0 Hz, 2H), 3.68 (q, J = 7.2 Hz, 2H), 1.40 (t, J = 6.9 Hz, 3H). ^{13}C NMR (75 MHz, DMSO-d_6, ppm) δ 185.8, 165.1, 140.7, 136.8, 136.1, 133.5, 130.0, 129.7, 48.0, 8.6. Elemental Analysis Calcd: C 45.36, H 3.81, Cl 11.16, N 4.41. Found: C 45.42, H 3.85, Cl 11.06, N 4.37, $C_{12}H_{12}ClNO_5S$. HPLC retention time: 29.9 min.

Computational Chemistry Methods. To study the interaction between compound **7c** and FTO, the previously reported FTO crystal structure (PDB code: 3LFM) was used as a docking model. Hydrogen atoms were added, while all water molecules and the substrate 3-methylthymine deoxyriboside were removed from the protein. Compound **7c** was initially sketched in MDL-ISIS/Draw and converted into 3D structure in SYBYL 6.9 with all proton and MMFF94 charges added. The compound was then minimized by Tripos Force Field in its default minimization set. Superposition of **7c** to *N*-oxalylglycine in the active site of FTO via the dihydroxy group leads to two binding models in opposite direction. One of the binding models was rejected since the phenyl ring of **7c** has a serious clash with the protein residue Leu203. The compound **7c** together with surrounding residues were minimized, and final binding model is shown in Figure 4.

Western Protocol. HeLa cells were grown at 37 °C with 5% CO_2 in Dulbecco's modified Eagle's medium (DMEM) supplemented with 5% fetal bovine serum (FBS) and 0.1 mM nonessential amino acids (Life Technologies, Carlsbad, CA). Cells were seeded into 100 mm culture dishes. When cell layers reached ∼80% confluence, the medium was replaced with OPTI-MEM (Life Technologies, Carlsbad, CA) and incubated for 24 h. Drug or vehicle control (1% DMSO) was then added to the existing medium, and incubation was continued overnight. Following incubation, the cells were washed twice in cold 1× phosphate buffered saline (PBS) and fractionated into cytoplasmic and nuclear fractions. Next, 30 μg of the nuclear fractions was resolved on 4−12% NuPage gels (Life Technologies, Carlsbad, CA), and proteins were transferred to nitrocellulose membranes. Standard immunoblotting procedures were performed. The blots were

developed using the ECL Plus Western detection kit (Thermo Scientific, Sunnyvale, CA).

FTO Enzyme Inhibition. The activity assay was performed as previously reported.[28,45] The reaction mixture contained the following components: DNA containing m^6A (5′-ATTGTCA(m^6A)CAG-CAGC-3′) (100 μM), FTO protein (30 μM), KCl (100 mM), $MgCl_2$ (2 mM), L-ascorbic acid (2 mM), α-ketoglutarate (300 μM), $(NH_4)_2Fe(SO_4)_2{\cdot}6H_2O$ (150 μM), and 50 mM HEPES buffer (pH 7.5). The reaction was incubated with the inhibitor at room temperature for 15 min, quenched by adding 5 mM EDTA, and followed by heating at 95 °C for 10 min. DNA was digested by nuclease P1 and alkaline phosphatase, and then analyzed on a HPLC system equipped with an Acclaim 120, C18, 5 μm Analytical column (4.6 × 150 mm) (Thermo Scientific, Sunnyvale, CA) eluted with buffer A (5 mM ammonia acetate) and buffer B (60% acetonitrile, 0.01% TFA, 5 mM ammonia acetate) with a flow rate of 1 mL min^{-1} at room temperature. The detection wavelength was set at 260 nm.

Cellular m^6A Quantification. The activity assay was performed as previously reported.[28,45] Total RNA was isolated from HeLa cells with TRAZOL Reagent (Life Technologies, Carlsbad, CA). mRNA was extracted using PolyATtract mRNA Isolation Systems (Promega, Madison, WI), followed by further removal of contaminated rRNA using the RiboMinus Transcriptome Isolation Kit (Life Technologies, Carlsbad, CA). mRNA concentration was measured via NanoDrop. The quality was analyzed using an Agilent 2100 bioanalyzer with an RNA NanoChip. A volume of 1 μg of mRNA was digested by nuclease P1 (2 U) in 40 μL of buffer containing 25 mM NaCl and 2.5 mM $ZnCl_2$ at 37 °C for 1 h, followed by the addition of NH_4HCO_3 (1 M, 3 μL) and alkaline phosphatase (0.5 U). After an additional incubation at 37 °C for 1 h, the solution was diluted 5 times, and 10 μL of the solution was injected into the LC-MS/MS instrument. The nucleosides were separated by reverse phase ultraperformance liquid chromatography on a C18 column, with online mass spectrometry detection using Agilent 6410 QQQ triple-quadrupole LC mass spectrometer in positive electrospray ionization mode. The nucleosides were quantified using the nucleoside to base ion mass transitions of 282 to 150 (m^6A) and 268 to 136 (A). Quantification was performed by comparison with the standard curve obtained from pure nucleoside standards running at the same batch of samples. The ratio of m^6A to A was calculated based on the calculated concentrations. Statistical analysis performed included the *t* test and calculation of the *p*-value.

MicroRNA Methods. HeLa cells were grown as described above in the Western Protocol subsection. mRNA was isolated from cells using miRvana (Life Technologies, Carlsbad, CA) and submitted to LC Sciences (Houston, TX) for analysis using a proprietary microRNA (miR Base version 19) microarray.

Anticonvulsant screening utilized standard animal models performed by the NIH/NINDS Anticonvulsant Screening Program as described on their Web site (http://www.ninds.nih.gov/research/asp/testdesc.htm).

AUTHOR INFORMATION

Corresponding Author

*Tel.: 623-572-3568. Fax: 623-572-3565. E-mail: molsen@midwestern.edu.

Author Contributions

G.Z. performed FTO isolation and inhibition assays, cell assays, and RNA isolation. T.C. synthesized compounds **5**, **6b** and **7c**. L.T. synthesized compounds **6e** and **7d**. G.Z.W. assisted in enzyme assays. P.I. assisted in the synthesis of all compounds. M.E.B. assisted in the characterization of compounds. G.J.G. analyzed spectra and assisted in proofing the manuscript. L.Z. performed computational models. N.B. performed western blot experiments and analysis. C.H. directed enzyme isolation, cell assays, and RNA isolation. J.R. and M.J.O jointly conceived the project and wrote the manuscript.

Funding

T.C. thanks the Midwestern University Kenneth Suarez Summer Fellowship program. M.E.B. and G.J.G. acknowledge the KSU CSM Mentor Protégé Research Program. J.R. and M.J.O. acknowledge support from Midwestern University – CPG. C.H. acknowledges NIH GM 071440.

Notes

The authors declare no competing financial interest.

ACKNOWLEDGMENTS

M.J.O. would like to acknowledge J. Barletta for assistance with statistical calculations.

ABBREVIATIONS

FTO, fat mass and obesity associated protein; m^6A, N^6-methyladenosine; PHD, prolyl-4-hydroxylase; KDM, lysine demethylase; FIH, factor inhibiting HIF; ASPH, aspartyl-(asparaginyl)-β-hydroxylase; TET-1, Ten eleven translocase-1; SVCT, sodium coupled vitamin C transporter; NOG, *N*-oxalylglycine; ASP, Anticonvulsant Screening Program; JMJD2A, Jumanji D2A; 2-OG, 2-oxoglutarate; miRNA, microRNA; Epo, erythropoietin; AED, antiepileptic drug; HIF, hypoxia inducible transcription factor

REFERENCES

(1) Rowles, J., and Olsen, M. (2012) Perspectives on the development of antioxidant antiepileptogenic agents. *Mini Rev. Med. Chem. 12*, 1015–1027.

(2) Pitkanen, A. (2010) Therapeutic approaches to epileptogenesis—hope on the horizon. *Epilepsia 51* (Suppl 3), 2–17.

(3) (2012) The NIH/NINDS Anticonvulsant Screening Program (ASP): Recommendations from the working group's 2012 review of the Program. *Epilepsia 53*, 1837–1839.

(4) Bialer, M., and White, H. S. (2010) Key factors in the discovery and development of new antiepileptic drugs. *Nat. Rev. Drug Discovery 9*, 68–82.

(5) Loscher, W. (2011) Critical review of current animal models of seizures and epilepsy used in the discovery and development of new antiepileptic drugs. *Seizure 20*, 359–368.

(6) Brines, M. L., Ghezzi, P., Keenan, S., Agnello, D., de Lanerolle, N. C., Cerami, C., Itri, L. M., and Cerami, A. (2000) Erythropoietin crosses the blood-brain barrier to protect against experimental brain injury. *Proc. Natl. Acad. Sci. U.S.A. 97*, 10526–10531.

(7) Chu, K., Jung, K. H., Lee, S. T., Kim, J. H., Kang, K. M., Kim, H. K., Lim, J. S., Park, H. K., Kim, M., Lee, S. K., and Roh, J. K. (2008) Erythropoietin reduces epileptogenic processes following status epilepticus. *Epilepsia 49*, 1723–1732.

(8) Miskowiak, K. W., Favaron, E., Hafizi, S., Inkster, B., Goodwin, G. M., Cowen, P. J., and Harmer, C. J. (2009) Effects of erythropoietin on emotional processing biases in patients with major depression: an exploratory fMRI study. *Psychopharmacology (Berlin, Ger.) 207*, 133–142.

(9) Miskowiak, K. W., Vinberg, M., Harmer, C. J., Ehrenreich, H., and Kessing, L. V. (2012) Erythropoietin: a candidate treatment for mood symptoms and memory dysfunction in depression. *Psychopharmacology (Berlin, Ger.) 219*, 687–698.

(10) Garcia, C. S. (2012) Depression in temporal lobe epilepsy: a review of prevalence, clinical features, and management considerations. *Epilepsy Res. Treat. 2012*, 809843.

(11) Sharp, F. R., and Bernaudin, M. (2004) HIF1 and oxygen sensing in the brain. *Nat. Rev. Neurosci. 5*, 437–448.

(12) Siddiq, A., Aminova, L. R., and Ratan, R. R. (2007) Hypoxia inducible factor prolyl 4-hydroxylase enzymes: center stage in the battle against hypoxia, metabolic compromise and oxidative stress. *Neurochem. Res. 32*, 931–946.

(13) Devi, P. U., Manocha, A., and Vohora, D. (2008) Seizures, antiepileptics, antioxidants and oxidative stress: an insight for researchers. *Exp. Opin. Pharmacother. 9*, 3169−3177.
(14) Tome, A. R., Feng, D., and Freitas, R. M. (2010) The effects of α-tocopherol on hippocampal oxidative stress prior to in pilocarpine-induced seizures. *Neurochem. Res. 35*, 580−587.
(15) Flashman, E., Davies, S. L., Yeoh, K. K., and Schofield, C. J. (2010) Investigating the dependence of the hypoxia-inducible factor hydroxylases (factor inhibiting HIF and prolyl hydroxylase domain 2) on ascorbate and other reducing agents. *Biochem. J. 427*, 135−142.
(16) Hopper, A. T., Witiak, D. T., and Ziemniak, J. (1998) Design, synthesis, and biological evaluation of conformationally constrained aci-reductone mimics of arachidonic acid. *J. Med. Chem. 41*, 420−427.
(17) Pernot, F., Heinrich, C., Barbier, L., Peinnequin, A., Carpentier, P., Dhote, F., Baille, V., Beaup, C., Depaulis, A., and Dorandeu, F. (2011) Inflammatory changes during epileptogenesis and spontaneous seizures in a mouse model of mesiotemporal lobe epilepsy. *Epilepsia 52*, 2315−2325.
(18) McDonough, M. A., Li, V., Flashman, E., Chowdhury, R., Mohr, C., Lienard, B. M., Zondlo, J., Oldham, N. J., Clifton, I. J., Lewis, J., McNeill, L. A., Kurzeja, R. J., Hewitson, K. S., Yang, E., Jordan, S., Syed, R. S., and Schofield, C. J. (2006) Cellular oxygen sensing: Crystal structure of hypoxia-inducible factor prolyl hydroxylase (PHD2). *Proc. Natl. Acad. Sci. U.S.A. 103*, 9814−9819.
(19) Warshakoon, N. C., Wu, S., Boyer, A., Kawamoto, R., Sheville, J., Renock, S., Xu, K., Pokross, M., Zhou, S., Winter, C., Walter, R., Mekel, M., and Evdokimov, A. G. (2006) Structure-based design, synthesis, and SAR evaluation of a new series of 8-hydroxyquinolines as HIF-1α prolyl hydroxylase inhibitors. *Bioorg. Med. Chem. Lett. 16*, 5517−5522.
(20) Dahn, H., Lawendel, J. S., Hoegger, E. F., and Schenker, E. (1954) Reductone. II. The isolation of 5-aryl-3-hydroxytetronimide from aromatic and heterocyclic-aromatic aldehydes, glyoxal, and potassium cyanide. *Helv. Chim. Acta 37*, 1309−1318.
(21) Pavan, B., Dalpiaz, A., Ciliberti, N., Biondi, C., Manfredini, S., and Vertuani, S. (2008) Progress in drug delivery to the central nervous system by the prodrug approach. *Molecules 13*, 1035−1065.
(22) Levy, R. H. (2002) *Antiepileptic drugs*, 5th ed., Lippincott Williams & Wilkins, Philadelphia.
(23) Brokers, N., Le-Huu, S., Vogel, S., Hagos, Y., Katschinski, D. M., and Kleinschmidt, M. (2010) Increased chemoresistance induced by inhibition of HIF-prolyl-hydroxylase domain enzymes. *Cancer Sci. 101*, 129−136.
(24) Ogle, M. E., Gu, X., Espinera, A. R., and Wei, L. (2012) Inhibition of prolyl hydroxylases by dimethyloxaloylglycine after stroke reduces ischemic brain injury and requires hypoxia inducible factor-1α. *Neurobiol. Dis. 45*, 733−742.
(25) Elkins, J. M., Hewitson, K. S., McNeill, L. A., Seibel, J. F., Schlemminger, I., Pugh, C. W., Ratcliffe, P. J., and Schofield, C. J. (2003) Structure of factor-inhibiting hypoxia-inducible factor (HIF) reveals mechanism of oxidative modification of HIF-1 alpha. *J. Biol. Chem. 278*, 1802−1806.
(26) Ng, S. S., Kavanagh, K. L., McDonough, M. A., Butler, D., Pilka, E. S., Lienard, B. M., Bray, J. E., Savitsky, P., Gileadi, O., von Delft, F., Rose, N. R., Offer, J., Scheinost, J. C., Borowski, T., Sundstrom, M., Schofield, C. J., and Oppermann, U. (2007) Crystal structures of histone demethylase JMJD2A reveal basis for substrate specificity. *Nature 448*, 87−91.
(27) Han, Z., Niu, T., Chang, J., Lei, X., Zhao, M., Wang, Q., Cheng, W., Wang, J., Feng, Y., and Chai, J. (2010) Crystal structure of the FTO protein reveals basis for its substrate specificity. *Nature 464*, 1205−1209.
(28) Jia, G., Fu, Y., Zhao, X., Dai, Q., Zheng, G., Yang, Y., Yi, C., Lindahl, T., Pan, T., Yang, Y. G., and He, C. (2011) N6-methyladenosine in nuclear RNA is a major substrate of the obesity-associated FTO. *Nat. Chem. Biol. 7*, 885−887.
(29) Aik, W., Demetriades, M., Hamdan, M. K., Bagg, E. A., Yeoh, K. K., Lejeune, C., Zhang, Z., McDonough, M. A., and Schofield, C. J. (2013) Structural basis for inhibition of the fat mass and obesity associated protein (FTO). *J. Med. Chem. 56*, 3680−3688.
(30) Chen, B., Ye, F., Yu, L., Jia, G., Huang, X., Zhang, X., Peng, S., Chen, K., Wang, M., Gong, S., Zhang, R., Yin, J., Li, H., Yang, Y., Liu, H., Zhang, J., Zhang, H., Zhang, A., Jiang, H., Luo, C., and Yang, C. G. (2012) Development of cell-active N6-methyladenosine RNA demethylase FTO inhibitor. *J. Am. Chem. Soc. 134*, 17963−17971.
(31) Jia, G., Yang, C. G., Yang, S., Jian, X., Yi, C., Zhou, Z., and He, C. (2008) Oxidative demethylation of 3-methylthymine and 3-methyluracil in single-stranded DNA and RNA by mouse and human FTO. *FEBS Lett. 582*, 3313−3319.
(32) Rowles, J., Wong, M., Powers, R., and Olsen, M. (2012) FTO, RNA epigenetics and epilepsy. *Epigenetics 7*, 1094−1097.
(33) Madsen, M. B., Birck, M. M., Fredholm, M., and Cirera, S. (2010) Expression studies of the obesity candidate gene FTO in pig. *Anim. Biotechnol. 21*, 51−63.
(34) Meyer, K. D., Saletore, Y., Zumbo, P., Elemento, O., Mason, C. E., and Jaffrey, S. R. (2012) Comprehensive analysis of mRNA methylation reveals enrichment in 3′ UTRs and near stop codons. *Cell 149*, 1635−1646.
(35) Dominissini, D., Moshitch-Moshkovitz, S., Schwartz, S., Salmon-Divon, M., Ungar, L., Osenberg, S., Cesarkas, K., Jacob-Hirsch, J., Amariglio, N., Kupiec, M., Sorek, R., and Rechavi, G. (2012) Topology of the human and mouse m6A RNA methylomes revealed by m6A-seq. *Nature 485*, 201−206.
(36) Bian, S., and Sun, T. (2011) Functions of noncoding RNAs in neural development and neurological diseases. *Mol. Neurobiol. 44*, 359−373.
(37) Jimenez-Mateos, E. M., and Henshall, D. C. (2013) Epilepsy and microRNA. *Neuroscience 238*, 218−229.
(38) Risbud, R. M., and Porter, B. E. (2013) Changes in microRNA expression in the whole hippocampus and hippocampal synaptoneurosome fraction following pilocarpine induced status epilepticus. *PLoS One 8*, e53464.
(39) Ho, A. J., Stein, J. L., Hua, X., Lee, S., Hibar, D. P., Leow, A. D., Dinov, I. D., Toga, A. W., Saykin, A. J., Shen, L., Foroud, T., Pankratz, N., Huentelman, M. J., Craig, D. W., Gerber, J. D., Allen, A. N., Corneveaux, J. J., Stephan, D. A., DeCarli, C. S., DeChairo, B. M., Potkin, S. G., Jack, C. R., Jr., Weiner, M. W., Raji, C. A., Lopez, O. L., Becker, J. T., Carmichael, O. T., Thompson, P. M., and Alzheimer's Disease Neuroimaging, I. (2010) A commonly carried allele of the obesity-related FTO gene is associated with reduced brain volume in the healthy elderly. *Proc. Natl. Acad. Sci. U.S.A. 107*, 8404−8409.
(40) Sobczyk-Kopciol, A., Broda, G., Wojnar, M., Kurjata, P., Jakubczyk, A., Klimkiewicz, A., and Ploski, R. (2011) Inverse association of the obesity predisposing FTO rs9939609 genotype with alcohol consumption and risk for alcohol dependence. *Addiction 106*, 739−748.
(41) Karra, E., O'Daly, O. G., Choudhury, A. I., Yousseif, A., Millership, S., Neary, M. T., Scott, W. R., Chandarana, K., Manning, S., Hess, M. E., Iwakura, H., Akamizu, T., Millet, Q., Gelegen, C., Drew, M. E., Rahman, S., Emmanuel, J. J., Williams, S. C., Ruther, U. U., Bruning, J. C., Withers, D. J., Zelaya, F. O., and Batterham, R. L. (2013) A link between FTO, ghrelin, and impaired brain food-cue responsivity. *J. Clin. Invest. 123*, 3539−3551.
(42) Hess, M. E., Hess, S., Meyer, K. D., Verhagen, L. A., Koch, L., Bronneke, H. S., Dietrich, M. O., Jordan, S. D., Saletore, Y., Elemento, O., Belgardt, B. F., Franz, T., Horvath, T. L., Ruther, U., Jaffrey, S. R., Kloppenburg, P., and Bruning, J. C. (2013) The fat mass and obesity associated gene (FTO) regulates activity of the dopaminergic midbrain circuitry. *Nat. Neurosci. 16*, 1042−1048.
(43) Liu, H., Roy, M., and Tian, F. F. (2013) MicroRNA-based therapy: a new dimension in epilepsy treatment. *Int. J. Neurosci. 123*, 617−622.
(44) Dahn, H., and v. Castelmur, H. (1956) Reductone. VII. Paper chromatography of 4-aryl-2-hydroxytetronimides and 5,6-diaryl-3,4,5-trihydroxy-5,6-dihydro-2-pyronimides. *Helv. Chim. Acta 39*, 1855−1858.

(45) Fu, Y., Dai, Q., Zhang, W., Ren, J., Pan, T., and He, C. (2010) The AlkB domain of mammalian ABH8 catalyzes hydroxylation of 5-methoxycarbonylmethyluridine at the wobble position of tRNA. *Angew. Chem., Int. Ed. 49*, 8885−8888.